XVIII International Conference on Water Resources
CMWR 2010
J. Carrera (Ed)

SENSITIVITY TO PARAMETERS IN NON-DARCY FLOW MODEL FROM PORESCALE THROUGH MESOSCALE

Małgorzata Peszyńska[†] and Anna Trykozko[‡] and Ken Kennedy[*]

[*†]Department of Mathematics, Oregon State University, Corvallis, OR, 97330, USA
[‡]ICM, University of Warsaw, Pawinskiego 5A, 02-106 Warszawa, Poland
e-mail: [†]mpesz@math.oregonstate.edu, [‡]aniat@icm.edu.pl, [*]kennedke@math.oregonstate.edu

Key words: porescale modeling, non-Darcy flow, inertia terms, upscaling, mesoscale

Summary. We consider flow with inertia at porescale and mesoscale and discuss sensitivity of flow results to the functional models and parameters.

1 INTRODUCTION

Until recently, computational modeling of flow in porous media has been constrained to the scales of physical observation, i.e., to the Darcy scale. In the last decade modeling of flow and transport phenomena at porescale has become feasible thanks to increases in computational power and many porescale *discrete* models such as pore network and lattice models were constructed.

In this paper we are interested in results of *continuum* porescale models of flow and specifically of flow with inertia, and in the sensitivity of mesoscale non-Darcy flow models to the parameters derived from porescale computations. In particular, we are interested in anisotropy and in the functional form of non-Darcy model; both are subject of current research and the topic of various controversies.

In previous work [1, 2, 3] we considered only the Forchheimer model for isotropic geometries; its upscaling [4] from mesoscale to macroscale and comparison to experiments [3]. Below we discuss derivation of parameters of a non-Darcy model from porescale and study sensitivity of that model at mesoscale.

2 PORESCALE TO MESOSCALE

We first provide an illustration of porescale computations. Then we discuss the parameteres of the upscaled non-Darcy flow model.

In [1, 2] we proposed a numerically sound computational method for computing flow conductivities from porescale experiments. We have tested the method on synthetic porescale geometries such as the one shown in Figure 1.

Consider the flow in porescale geometry with a small flow rate; upscaling the results

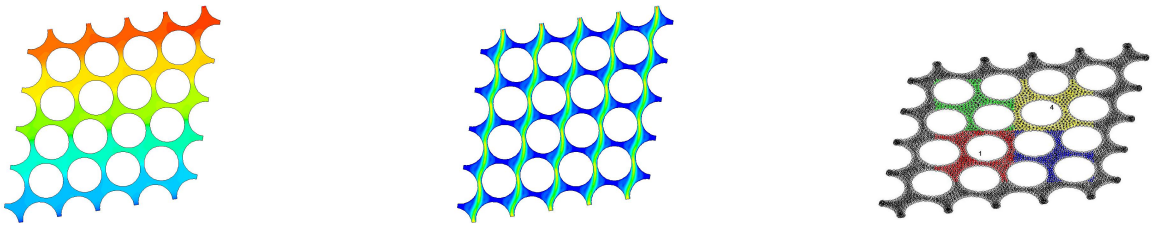

pressure field **magnitude of velocity** **averaging regions**

Figure 1: Computational results at porescale and region of upscaling

[5] allows to compute conductivity $\mathbf{K}$ or resistivity $\mathbf{K}^{-1}$ in Darcy's law

$$\mathbf{K}^{-1}\mathbf{u} = -\nabla p. \tag{1}$$

Computationally, we set up at least two independent experiments $l = 1, 2$ with general flow directions independent from one another. We superimpose a mesoscale grid, see the regions $\Omega_k, k = 1, 2, 3, 4$ in Figure 1, and compute averages of pressures and of velocities. For $l = 1$ we average the pressures over $\Omega_{1\cup 3} := \Omega_1 \cup \Omega_3$ and $\Omega_{2\cup 4}$; this way we get the first component of the pressure gradient. We proceed similarly for other components and $l = 2$. Then we match velocities to pressures and obtain $\mathbf{K}$ as the coefficient of proportionality in (1); details are provided in [1, 2]. The momentum equation (1) must be complemented by conservation of mass $\nabla \cdot \mathbf{u} = 0$ plus appropriate boundary conditions in order to obtain a solution at mesoscale.

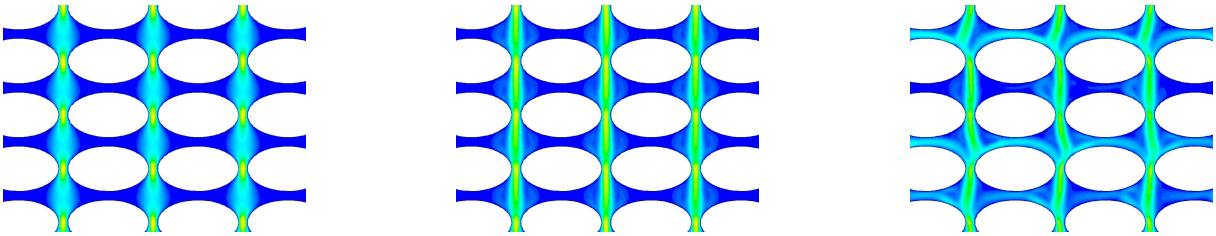

$\mathbf{Re}(|\mathbf{u}^{(1)}|) = 0.1$ $\mathbf{Re}(|\mathbf{u}|^{(2)}) = 1$ $\mathbf{Re}(|\mathbf{u}|^{(3)}) = 5$

Figure 2: Flow at porescale in anisotropic geometry which results in anisotropic diagonal κ. Shown are three experiments $j = 1, 2, 3$. Results $j = 3$ appear unresolved at the grid used; however, this has little bearing upon averaged results.

Next we extend this idea to flow with inertia. Consider additional experiments numbered $j = 2, \ldots$ corresponding to increasing flow rates parameterized by Reynolds number $\mathbf{Re}$. For each $j \in \mathbf{J}$ we obtain $\mathbf{u}^{(j)}$ and the coefficient of proportionality, the resistance $(\kappa^{-1})^{(j)}$. As postulated in [6, 7, 8, 9] and shown by our computational experiments in Figure 3, the resistance κ^{-1} increases with flow rates. We seek a functional model for $\kappa^{-1}(|\mathbf{u}|)$; first we are concerned with a power model and next with anisotropy.

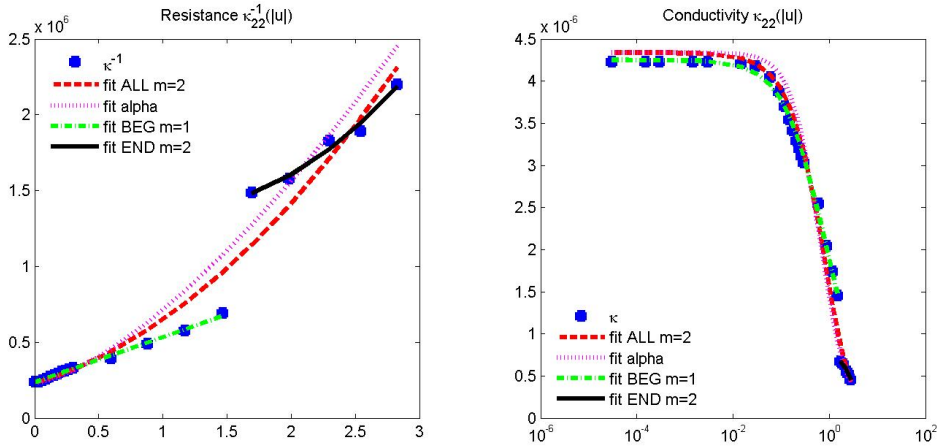

Figure 3: Fitting κ: linear scale (left) and logarithmic scale (right)

2.1 Fitting results to non-Darcy model with various powers

The scalar non-Darcy model at mesoscale extending (1) is

$$\kappa^{-1}(|\mathbf{u}|)\mathbf{u} = -\nabla p \tag{2}$$

where in the scalar case $\kappa^{-1}(|\mathbf{u}|)$ takes one of functional forms

$$\kappa_1^{-1}(|\mathbf{u}|) \approx K_1^{-1} + \beta_1|\mathbf{u}| \tag{3}$$
$$\kappa_2^{-1}(|\mathbf{u}|) \approx K_2^{-1} + \beta_2|\mathbf{u}| + \gamma_2|\mathbf{u}|^2 \tag{4}$$
$$\kappa_\alpha^{-1}(|\mathbf{u}|) \approx K_0^{-1} + \beta_\alpha|\mathbf{u}|^\alpha. \tag{5}$$

At mesoscale we additionally consider

$$\kappa_{2,0}^{-1}(|\mathbf{u}|) \approx K_0^{-1} + \gamma_{2,0}|\mathbf{u}|^2. \tag{6}$$

We note that (3) is the Forchheimer model [6] and (4), (6) are the cubic models discussed in [10, 11]. The choice of models is motivated by discussions and controversies brought up in [10, 12, 11, 13]. See also [8, 14] for (6).

We discuss fitting of $(\kappa^{-1}(|\mathbf{u}|))^{(j)}$ to one of the models above; we use κ_m^{-1} to denote the highest exponent m in $|\mathbf{u}|^m$ unless this exponent is sought itself and called α. First, we generally expect that as $|\mathbf{u}| \to 0$, we have $\kappa^{-1}(|\mathbf{u}|) \to K^{-1}$. We assume that it suffices to take as $\mathbf{K}$ the first of the computed values $K_0^{-1} := (\kappa^{-1})^{(1)}$. Next, we observe that while κ decreases with $|\mathbf{u}|$, the rate of this decrease appears different in two regimes: for small j and for large j. These regimes are dubbed BEG and END respectively below, we attempt different fits in each regime.

Results are summarized in Table 1 and illustrated in Figure 3. They generally show that the Forchheimer model is not a good fit for the entire range $j \in \mathbf{J}$, as was discussed

in [11]. Overall, a better fit is provided with noninteger power $\alpha \approx 1.5$ or with separate models depending on the regime.

model	K_0^{-1}	β	γ	α	δ
	Component κ_{11}^{-1}, value $K_0^{-1} = (\kappa^{-1})^{(1)} = 220775$				
κ_1^{-1}	148566	631759		m=1	0.764550
κ_2^{-1}	214099	228756	168599	m=2	0.642016
$\kappa_{1,BEG}^{-1}$	216648	293008		m=1	0.049507
$\kappa_{2,END}^{-1}$	2279880	-1.1522e+006	385123	m=2	0.181215
κ_α^{-1}		445393		1.47912	0.372862
$\kappa_{\alpha,BEG}^{-1}$		443105		1.47838	0.42205
$\kappa_{\alpha,END}^{-1}$		779032		0.789443	0.062347
	Component κ_{22}^{-1}, value $K_0^{-1} = (\kappa^{-1})^{(1)} = 337925$				
κ_1^{-1}	226949	1.98132e+006		m=1	0.539661
κ_2^{-1}	253086	1.82059e+006	67243.2	m=2	0.588369
$\kappa_{1,BEG}^{-1}$	326711	1.10484e+006		m=1	0.092334
$\kappa_{2,END}^{-1}$	1090060	1.05541e+006	234183	m=2	0.783017
κ_α^{-1}		1.77981e+006		1.44333	0.359917
$\kappa_{\alpha,BEG}^{-1}$		2.30166e+006		1.49688	0.361737
$\kappa_{\alpha,END}^{-1}$		2.00719e+006		0.947317	0.077736

Table 1: Fitting different models to upscaled results of porescale computations. Last column shows the maximum relative deviation from the model

2.2 Fitting anisotropic porescale results

The original models [6, 7] dealt with scalar extensions of (1) to (2). Since $\mathbf{K}$ is in general anisotropic, a natural question is how the functional models of κ should account for anisotropy. See [10, 11] for relevant discussion. Since it may be difficult to get any inertia parameters and in particular those of any anisotropic models from experiments [3], we discuss how to get them from computations at porescale.

The algorithm sketched above delivers, in general, four components of the tensor $(\kappa^{-1}(|\mathbf{u}|))^{(j)}$. Actually, up to computational error, the off-diagonal terms of $\mathbf{K}$ and of κ should be equal since the tensor is expected to be symmetric; this was confirmed in [2]. Now we assume that the off-diagonal values of κ are negligible; the general case will be discussed elsewhere. In other words, we assume that the main directions of flow are aligned with the principal axis of κ. At porescale, we can hypothesize that this is the case, e.g, for the flow experiment and geometry in Figure 2. Anyway, in this case, to fit $(\kappa^{-1}(|\mathbf{u}|))^{(j)}$ to $|\mathbf{u}|^{(j)}$ it is enough to separate the coordinate directions and fit separately the κ_{11}^{-1} and κ_{22}^{-1} components of κ^{-1}.

Results of fitting are shown in Table 1. They confirm that K_{11} appears larger than K_{22} as there is less dissipation along the elliptical lenses than across them. Most importantly, the results show that an anisotropic model for κ is necessary, albeit a simple one suffices in this case. We obtain $\beta_{11} \neq \beta_{22}$ in each model. In addition, β_{11} appears significantly smaller than β_{22}; this behavior agrees qualtiateively with experimental correlations in [15].

3 SENSITIVITY OF NON-DARCY MODEL AT MESOSCALE

At mesoscale, a non-Darcy model is cumbersome due to its interesting structure. In 1D, the Forchheimer model (3) can be resolved analytically [4]. However, a general discretization of (2) in 2D requires two levels of Newton iteration to obtain pressures and velocities. For some stencils simplified variants exist thanks to iteration-lagging [4] and allow the inner iteration to be resolved locally. However, not all can be extended to full anisotropy and general κ. We now have a global inner solver which honors anisotropy and possibly full tensor; details will be shown elsewhere.

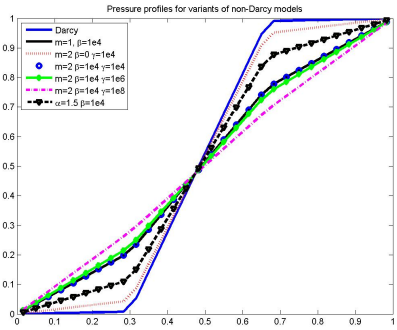

Figure 4: Computational results at mesoscale, heterogeneous 1D case.

Now we discuss the sensitivity of solutions to the parameters of non-Darcy flow. In general, solutions to PDEs may not be necessarily differentiable with respect to its parameters. However, in some simple cases one can explicitely compute the sensitivities i.e. derivatives of the quantity of interest with respect to each parameter.

For example, consider a 1D example of a homogeneous core in which conductivity K is constant and in which pressure is subject to Dirichlet boundary conditions at $x = 0, x = 1$. Consider also the case of a heterogeneous core with conductivities $1, 10^{-2}, 1$ assigned each to 1/3 of the core; see the pressure plots in Figure 4 and the values of fluxes in Table 2 computed for different models of κ and parameter values. For homogeneous $\mathbf{K}$ the pressure solution $p(x) = x$ regardless of functional model. However, u depends on the model. In some cases it can be computed explicitely [4].

Even if we cannot compute u explicitely, we can formally consider sensitivity of u with

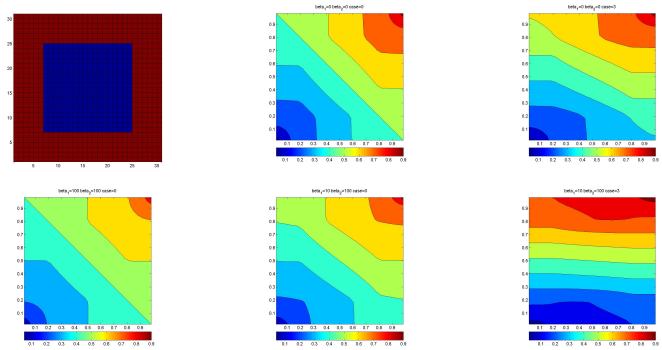

Figure 5: Computational results at mesoscale (heterogeneous 2D). Top row, from left: conductivity field, pressure profiles for isotropic Darcy case, and anisotropic Darcy case. Bottom row: pressure profiles for nonDarcy case. From left: isotropic K and $\beta = [1e2, 1e2], \beta = [1e1, 1e2]$, anisotropic $\beta = [1e1, 1e2]$

(1)	(3)	(6)	(4)	(4)	(4)	(5)
	$\beta = 1e4$	$\beta = 0$	$\beta = 1e4$	$\beta = 1e4$	$\beta = 1e4$	$\beta = 1e4$
	$\gamma = 0$	$\gamma = 1e4$	$\gamma = 1e4$	$\gamma = 1e6$	$\gamma = 1e8$	$\alpha = 1.5$
Homogeneous $K = 1$						
1.0000	0.0100	0.0457	0.0099	0.0075	0.0021	0.0249
Heterogeneous $K = [1, 1e-2, 1]$						
0.0268	0.0083	0.0234	0.0083	0.0067	0.0021	0.0169

Table 2: Fluxes for variants of non-Darcy model for homogeneous K and heterogeneous K in 1D. Shown are the values of fluxes $|\mathbf{u}|$ computed for different variants of κ given by (1), (3), (6), (4) with several parameters, and (5)

respect to parameters. This is done using implicit function theorem. Consider for example the power model (5) for non-Darcy flow set up as follows, with D in place of $\nabla p = p_x$

$$f(u, K, \alpha, \beta, D) = K^{-1}u + \beta|u|^{\alpha}u + D = 0 \tag{7}$$

In order to compute $\frac{\partial u}{\partial K}$ i.e. sensitivity of u with respect to K, we can differentiate (7) and compute formally $\frac{\partial f}{\partial K}$. Next we can solve for $\frac{\partial u}{\partial K}$.

A similar procedure can be followed for sensitivity with respect to β, α. We obtain

$$\frac{\partial u}{\partial K} = u\left(K + K^2\beta\alpha u|\mathbf{u}|^{\alpha-1}sgn(u) + K^2\beta|u|^{\alpha}\right)^{-1}, \tag{8}$$

$$\frac{\partial u}{\partial \beta} = -u|u|^{\alpha}\left(K^{-1} + \beta\alpha u|u|^{\alpha-1}sgn(u) + \beta|u|^{\alpha}\right)^{-1}, \tag{9}$$

$$\frac{\partial u}{\partial \alpha} = -\beta u|u|^{\alpha}\ln|u|\left(K^{-1} + \beta\alpha u|u|^{\alpha-1}sgn(u) + \beta|u|^{\alpha}\right)^{-1}. \tag{10}$$

These expressions give sensitivities at every point x at which we know u.

We can now analyze qualitative behavior of sensitivities with respect to one parameter depending on others. In particular, we find that when K increases from 1 to $1e3$, sensitivity to β increases somewhat by a small factor ≈ 1.2 while sensitivity to α increases by a factor of 2. These scaling factors do not depend linearly on the change in K. For example, if K decreases from 1 to .1, sensitivity to α decreases by a factor of 100, and the one to β decreases by a factor of 10.

These results are easily explained. When K is small, the flow rates are small and the value of velocity is relatively insensitive to a particular non-Darcy model. However, for large K and large flow rates, sensitivity to every parameter is larger.

Finally, we are interested in the profiles of pressures in 2D depending on anisotropic non-Darcy model; see Figure 5. Overall, it appears that the variations in pressures are more sensitive to anisotropy than they are to actual values of β. Our other experiences, also with upscaling of β [4], confirm that pressure solutions and total fluxes do not depend strongly on a particular value of β, as long as these do not vary more than by several orders of magnitude.

4 CONCLUSIONS

We have discussed a general methodology to use a virtual computational laboratory at porescale to compute flow parameters for a model with inertia at mesoscale. We have shown that the Forchheimer model may not be appropriate for the entire range of flow rates. However, it appears that the sensitivity of flow results at mesoscale to the choice of functional model or to its parameters is not strong, at least as compared to its dependence on conductivities. Further analysis including transport problems in a medium with large flow rates is underway.

The research of Peszynska and Kennedy was partially supported from NSF grant 0511190 and DOE grant 98089. Peszyńska was also partially supported as the Fulbright Research Scholar 2009-2010. We used computational facilities at ICM (Sun Constellation System with AMD Quad-Core Opteron 835X processors) as well as the facilities at Oregon State University including the COE cluster.

REFERENCES

[1] Malgorzata Peszynska, Anna Trykozko, and Kyle Augustson. Computational upscaling of inertia effects from porescale to mesoscale. In G. Allen, J. Nabrzyski, E. Seidel, D. van Albada, J. Dongarra, and P. Sloot, editors, *ICCS 2009 Proceedings, LNCS 5544, Part I*, pages 695–704, Berlin-Heidelberg, 2009. Springer-Verlag.

[2] M. Peszyńska and A. Trykozko. Convergence and stability in upscaling of flow with inertia from porescale to mesoscale. *Int. J. Multiscale Comput. Eng.*, (to appear), 2010.

[3] M. Peszyńska, A. Trykozko, and W. Sobieski. Forchheimer law in computational and experimental studies of flow through porous media at porescale and mesoscale. In *Current Advances in Nonlinear Analysis and Related Topics*, volume 32 of *GAKUTO Internat. Ser. Math. Sci. Appl.*, pages 463–482, 2010.

[4] C.R. Garibotti and M. Peszyńska. Upscaling non-Darcy flow. *Transport in Porous Media*, 80:401–430, 2009. published online March 13.

[5] Luc Tartar. Incompressible fluid flow in a porous medium–convergence of the homogenization process. In *Nonhomogeneous media and vibration theory*, volume 127 of *Lecture Notes in Physics*, pages 368–377. Springer-Verlag, Berlin, 1980.

[6] P. Forchheimer. Wasserbewegung durch Boden. *Zeit. Ver. Deut. Ing.*, (45):1781–1788, 1901.

[7] S. Ergun. Fluid flow through packed columns. *Chemical Engineering Progress*, 48:89–94, 1952.

[8] Adrian E. Scheidegger. *The physics of flow through porous media*. Revised edition. The Macmillan Co., New York, 1960.

[9] Jacob Bear. *Dynamics of Fluids in Porous Media*. Dover, New York, 1972.

[10] C. C. Mei and J.-L. Auriault. The effect of weak inertia on flow through a porous medium. *J. Fluid Mech.*, 222:647–663, 1991.

[11] Tiziana Giorgi. Derivation of Forchheimer law via matched asymptotic expansions. *Transport in Porous Media*, 29:191–206, 1997.

[12] M. Fourar, R. Lenormand, M. Karimi-Fard, and R. Horne. Inertia effects in high-rate flow through heterogeneous porous media. *Transport in Porous Media*, 60:353–370(18), September 2005.

[13] Alain Bourgeat, Eduard Marusić-Paloka, and Andro Mikelić. Weak nonlinear corrections for Darcy's law. *Math. Models Methods Appl. Sci.*, 6(8):1143–1155, 1996.

[14] S. Majid Hassanizadeh and W. Gray. High velocity flow in porous media. *Transport in Porous Media*, 2:521–531, 1987.

[15] S.C. Jones. Using the inertial coefficient beta to characterize heterogeneity in reservoir rock. In *SPE 16949*, 1987.